

The correlation analysis between electron density fluctuation and RF stray power in the CPD electron cyclotron plasma

Tomofumi RYOKAI¹, Hideki ZUSHI², Tomohiro MORISAKI³, Hiroshi IDEI²

Kazuaki HANADA², Kousuke DONO¹, Takashi MUTOH³, Shin KUBO³, Kazunobu NAGASAKI⁴

CPD experiment group²

1) *Interdisciplinary Graduate School of Engineering Science, Kyushu University Kasuga, Fukuoka 816-8580, Japan,*

2) *RIAM, Kyushu University, Kasuga, Fukuoka 816-8580, Japan,*

3) *NIFS, 322-6 Oroshi, Toki, Gifu 50-5292, Japan,*

4) *Kyoto University Yosidahonmati Sakyou Kyoto 606-8501, Japan,*

Corresponding author's e-mail: ryokai@triam.kyushu-u.ac.jp

(Received: 20 November 2009 / Accepted: 18 March 2010)

The two dimensional profiles of electron density and density fluctuation were measured in a slab-annular plasma by using Li beam probe method in CPD. The plasma was produced by electron cyclotron heating (ECH). The measurements were performed at the region, which include the cyclotron resonance R_{res} and the cut-off R_{RC} layers. The effects of the density fluctuation on the conversion from the electron cyclotron waves to the electron Bernstein waves are also investigation by studying cross correlation between the density fluctuations and the RF stray power, which are reflected from the cutoff layer. The vertical magnetic field is scanned with keeping the density scale length ~ 0.04 m, and its effects on the fluctuation and correlation are investigated. Although the coherent mode at $f=1.4$ kHz is found to extend between two layers at $B_z=0$ mT, the square cross coherency less than 0.2 is obtained. However, when B_z is 2.2 mT, the relative density fluctuation is reduced by 5 % but its existence region of the mode at $f=1.7$ kHz is discrete along the radius. The square cross coherency shows the radial dependence from 0.3 at R_{res} to 0.8 at R_{RC} suggesting the strong correlation between the density fluctuation and RF stray power near the cutoff layer.

Keywords: Spherical Tokamak, Li beam emission spectroscopy, Density fluctuation, Electron Bernstein wave Mode Conversion efficiency, RF stray power

1. Introduction

Electron cyclotron resonance (ECR) heating is very effective method to heat the magnetically confined plasma. For heating the plasma EC waves have to reach the ECR layer. However, the accessible electron density of plasma is limited by a cutoff density. When the cutoff layer exists in front of ECR layer, the EC waves are reflected by cutoff layer and cannot reach the ECR layer. On the other hand, a possibility for overcoming the density limit is the O-X-B or X-B mode conversion process proposed [1]. Here O, X, and B represent the ordinary, extraordinary, and electrostatic mode, the so-called electron Bernstein mode (EBW). Since EBW has no cutoff layer and is absorbed by electron cyclotron damping, the mode conversion process is one of candidate methods for heating and current drive in over-dense plasma [2].

The conversion efficiency η_{XB} from X to B or transmission efficiency T_{OX} from O to X mode at the cutoff layer strongly depends on the density scale length $L_n = n_e / |\partial n_e / \partial r|$ at the cutoff layer. In order to achieve high η_{XB} the short L_n of ~ 5 mm is required [3]. This was achieved by inserting a partial limiter from the low field side and the plasma heating was observed. In ref. [4] the steep density gradient obtained in H-mode was used to

achieve higher mode conversion efficiency, which was evaluated by analyzing of the DC component of RF power reflected by the cutoff layer.

It has been well known that the steep density gradient ∇n_e drives density fluctuations in the toroidal device. The effect of density fluctuations on O-X mode conversion efficiency was studied by assuming density fluctuations propagating in the poloidal direction. Model calculations showed that T_{OX} is reduced ~ 0.2 at the fluctuation amplitude \tilde{n}_e/n_e of ~ 0.1 at the poloidal correlation length of ~ 0.02 m [5]. The effects of the density fluctuation on η_{XB} have been studied by measuring EBW emission near from the upper hybrid resonance UHR layer [6]. 70 % anticorrelation between density and emission fluctuations was observed local to the UHR layer within 0.02 m. Correlation was not seen on either side of the UHR layer.

How is the conversion efficiency varied as a function of \tilde{n}_e/n_e when L_n is kept almost constant? For example, it has been reported that drift and flute modes in torus plasma can be stabilized by field line tying and magnetic shear[7,8]. This has been demonstrated by applying additional helical field on the simple mirror field [9].

In the spherical tokamak device CPD (Compact

author's e-mail: ryokai@triam.kyushu-u.ac.jp

Plasma wall interaction experimental Device), the non-inductive current drive experiments have been performed in hydrogen plasma using electron cyclotron waves [10]. The correlation between the density and RF stray power fluctuations are studied in a simple torus configuration with B_z and B_T magnetic field. Since annular-slab plasma, whose cut off layer extends vertically from the bottom to top walls, is produced at the low power level, the injected RF waves are expected to be reflected by the vertically elongated cutoff layer. The reflected power can be measured by diode detectors around the torus. By varying B_z/B_T line tying stabilization of the density fluctuations has been observed. \tilde{n}_e/n_e is reduced from 30-40 % at $B_z=0$ T to 10 % at $B_z=2$ mT. In this experiment L_n is observed to be almost constant [11]. The purpose of this paper is to investigate 1) the B_z stabilizing effect on low frequency coherent modes, and 2) correlation between density and RF stray power fluctuations.

The experimental set-up and diagnostics related with this paper will be described in Section 2. Stabilization of density fluctuation and correlation will be discussed in section 3. Finally the brief summary will be given in section 4.

2. Experimental setup and diagnostics

CPD is a spherical tokamak device whose diameter as well as height is ~ 1.2 m, as shown in Fig.1.

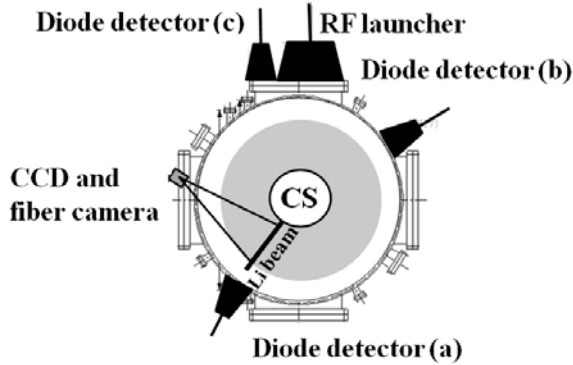


Fig.1 Top view of CPD

The major and minor radii are 0.3 and 0.2 m, respectively. The diameter of the center stack is 0.255 m. Four toroidal field coils and three sets of poloidal coils are used in this experiment. The decay index $n = -B_z/R (dB_z/dR)$ is almost fixed ~ 0.046 at $R=0.2$ m and the ratio B_z/B_T is varied 0.1. The plasma current and magnetic flux are measured by a Rogowski coil and 45 loops installed inside the chamber. T_e is measured by a scanning Langmuir probe [12]. RF waves ($f=8.2$ GHz and $P_{rf}=1\sim 70$ kW) are injected 0.01 m below the midplane at toroidal angle $\phi=0$ and both polarization modes (X and O) are injected through the horn antennas. The ECR plasma was produced at the electron

cyclotron resonance layer R_{res} of 0.16~0.19 m.

The stray RF power is detected by diode detectors with horns and attenuators at three locations around the torus. Here the present analysis is done for the detector B located at $\phi=302^\circ$, 0.2 m above the mid plane. The receiving angle of the horn is ~ 30 degree at FWHM and selectivity width of the electric field is $\sim 10^\circ$ at FWHM. Data are recorded at 1 MHz (Fig.2).

The electron density is measured by a thermal lithium beam [13~17]. In order to measure the two dimensional image of LiI(670.8 nm) a sheet Li beam whose radial width of ~ 0.3 m and toroidal width of 0.04 m is used. The beam is injected at $\phi=148^\circ$ from the bottom of the chamber. By analyzing the LiI intensity image detected by a CCD camera $n_e(R, Z)$ is measured and fifty photomultiplier tube (PMT) arrays coupled to a fiber array are used to study the density fluctuation $\tilde{n}_e(R, Z)$. Data are recorded at 300 kHz (Fig.2). The special resolutions are ~ 1 mm for CCD and 5 mm for PMT, respectively.

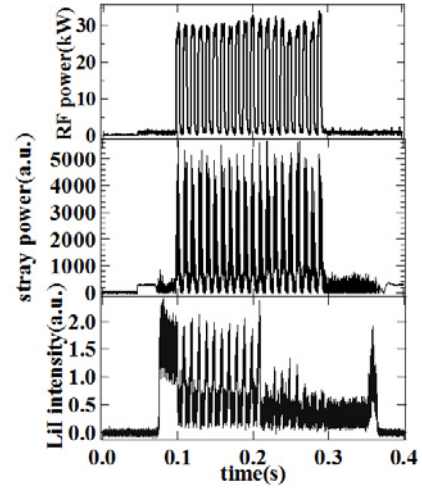


Fig.2 Time evolution of RF power, stray power and LiI intensity.

3. Experimental results

3-1. Density profile

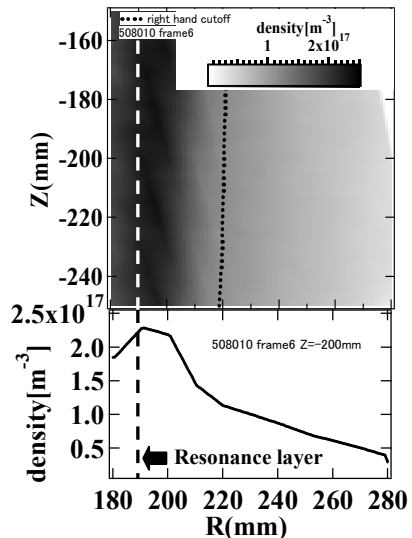


Fig.3 top: $n_e(R, Z)$ $R_{res}=191$ mm, bottom: $n_e(R, Z=-200\text{mm})$

Two dimensional (2D) density image $n_e(R, Z)$ and the radial profile $n_e(R, -200 \text{ mm})$ are shown in Fig.3. The breakdown occurred at $R_{\text{res}} = 0.19 \text{ m}$. The peak of density exists at R_{res} and plasma extends to the vertical direction. Thus a clear annular plasma is formed. The X-mode right hand cut-off layer (R_{CL}) exists at $R = 0.22 \sim 0.23 \text{ m}$. No or small effect of B_z on $n_e(R, Z)$ is seen and L_n is $\sim 40 \text{ mm}$ at R_{CL} . Since the R_{CL} extends vertically, the X-mode waves injected from the low field side cannot reach the resonance layer [14].

3-2. Fluctuations without B_z

Characteristics of density fluctuations in annulus plasma are investigated without B_z . In the region of $R < R_{\text{res}}$, $\vec{\nabla} n \cdot \vec{\nabla} B < 0$ and flute modes are expected to be stable. For $R > R_{\text{res}}$, however, since the density decays radially parallel to the effective gravity where the condition $\vec{\nabla} n \cdot \vec{\nabla} B > 0$, flute modes become unstable [18]. In this region where the density gradient exists the drift modes are expected to be unstable. The \tilde{n}_e/n_e measured by LiI relative amplitude $\tilde{I}_{\text{Li}}/I_{\text{Li}}$ is about 30 % around the expected mode conversion layer. The auto power spectrum S_{xx} and square cross coherency $\gamma_z^2(R = 0.22 \text{ m})$ at two points separated by the vertical distance of $\Delta Z \sim 0.025 \text{ m}$ is analyzed by fast Fourier transform FFT, as shown in Fig.4. The time window is $\sim 10 \text{ ms}$ and moving average at every 3.4 ms (1024 data points) is used. The frequency resolution is 0.3 kHz .

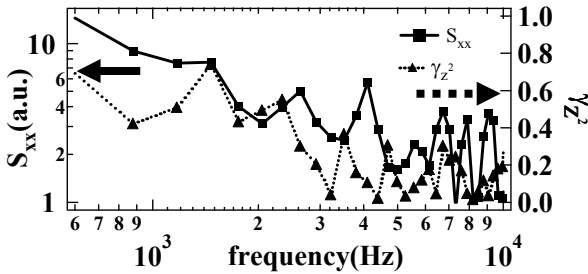


Fig.4 S_{xx} (solid line) and γ_z^2 (dotted line) spectra at $B_z = 0 \text{ T}$

S_{xx} shows a broadband spectrum with having several peaks in the frequency range of 1 to 10 kHz. Below 2.6 kHz high coherence > 0.4 is seen, especially $\gamma_z^2 \sim 0.8$ at $f \sim 1.4 \text{ kHz}$. This mode at $f = 1.4 \text{ kHz}$ is extended both in the viewing area of 50 mm in R and 25 mm in Z directions. The radial and vertical profiles of γ^2 are shown in Fig.5.

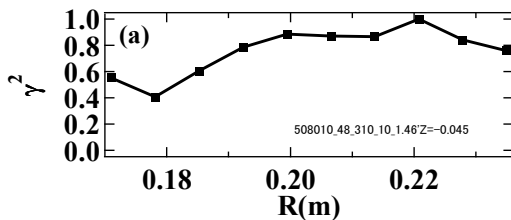


Fig.5 (a) Radial profiles of γ^2 ($f = 1.46 \text{ kHz}$) at $Z = -0.04 \text{ m}$

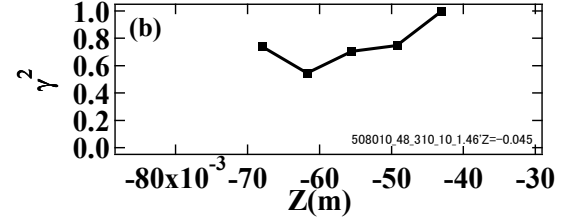


Fig.5 (b) Vertical profiles of γ^2 ($f = 1.46 \text{ kHz}$) at $R = 0.22 \text{ m}$

The radial correlation length ($1/e$ distance of the coherency) for this mode is considered to be longer than the viewing scales. The radial and vertical profiles of cross phase θ_R and θ_Z at $f = 1.4 \text{ kHz}$ are shown in Fig.6. The radial phase velocity determined by a relation $2\pi f(\Delta R/\theta_R)$ is about 700 m/s .

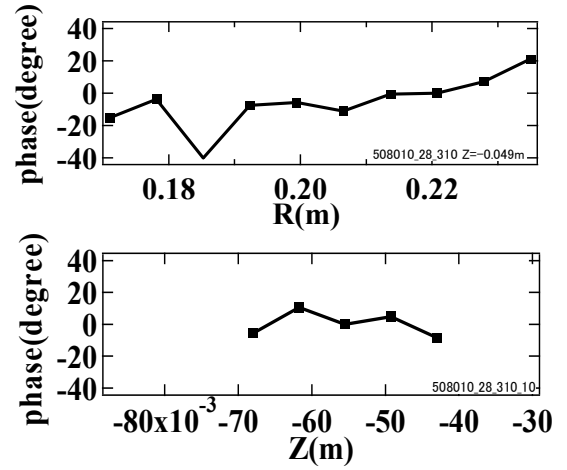


Fig.6 Radial and vertical profiles of phase ($f = 1.46 \text{ kHz}$) at $Z = -0.05 \text{ m}$, and $R = 0.22 \text{ m}$, respectively

3-3. Fluctuation with B_z

In this section how the B_z affects the density fluctuations will be presented. The \tilde{n}_e/n_e is reduced to ~ 0.2 at $B_z = 2.2 \text{ mT}$ at R_{res} . The characteristics of the fluctuations are drastically changed. The S_{xx} and γ_z^2 spectra are shown in Fig.7.

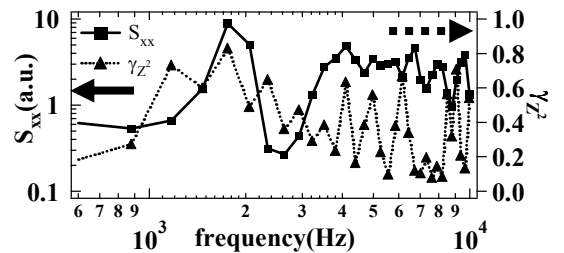


Fig.7 S_{xx} (solid line) and γ_z^2 (dotted line) spectra at $B_z = 2.2 \text{ mT}$

In the low frequency range ($f < 2$ kHz) the broadband spectrum at $B_z = 0$ mT is changed to a relatively narrow peak at $f \sim 1.7$ kHz, whose width < 1 kHz. The γ_z^2 at this peak is reduced from 0.8 to 0.6. The integrated power in the low frequency range ($f < 10$ kHz) was reduced to 0.47 of that at $B_z = 0$ mT. The frequency averaged γ_z^2 is also reduced. The radial and vertical profiles of γ^2 at $f = 1.7$ kHz are shown in Fig.8.

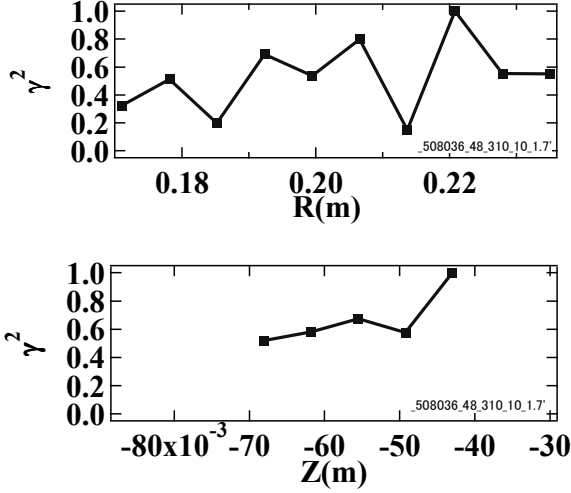


Fig.8 Radial and vertical profile of γ^2 ($f=1.7$ kHz) at $Z=-0.04$ m, and $R=0.22$ m, respectively

The γ^2 profile at $f=1.7$ kHz shows that the mode is extended to the vertical direction but is partially isolated in the radial direction. The radial correlation length is considered to be less than 0.03 m. The vertical profile of θ_z at $f=1.7$ kHz is shown in Fig.9. The variation in θ_z is within $\pm 20^\circ$ at $f=1.7$ kHz, suggesting that fluctuations propagate in phase near R_{RC} .

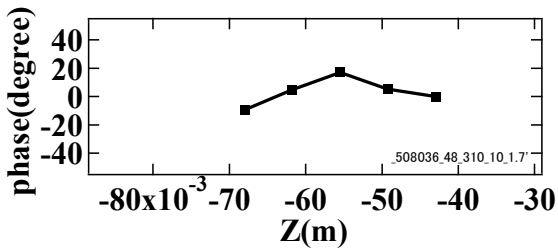


Fig.9 Vertical profile of phase ($f=1.7$ kHz) at $R=0.22$ m

3-4. Correlation between density fluctuation and RF stray power

At the $B_z=0$ mT, the auto power spectrum of RF stray signal (S_{yy}) and square coherency spectrum ($\gamma_{rf-dens}^2$) between the fluctuation component of RF stray power and \tilde{n}_e are shown in Fig10. S_{yy} is a broadband one similar to S_{xx} and these two signals are incoherent below $< \sim 7$ kHz. Figure 11 shows that radial and vertical profiles of $\gamma_{Z(rf-dens)}^2$ and $\gamma_{R(rf-dens)}^2$ at $f=1.4$ kHz are less than 0.2.

author's e-mail: ryokai@triham.kyushu-u.ac.jp

Although the coherence mode at $f=1.4$ kHz exists in density fluctuations, no correlation is found in fluctuating stray power.

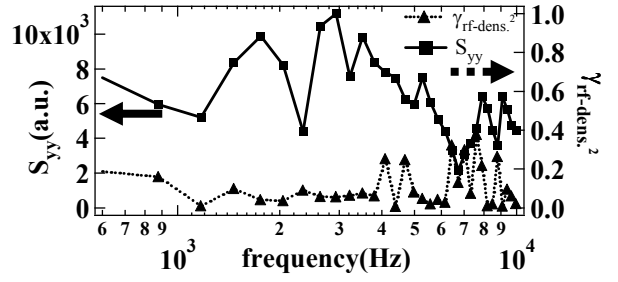


Fig.10 S_{yy} (solid line) and $\gamma_{rf-dens}^2$ (dotted line) spectra at $B_z=0$ mT.

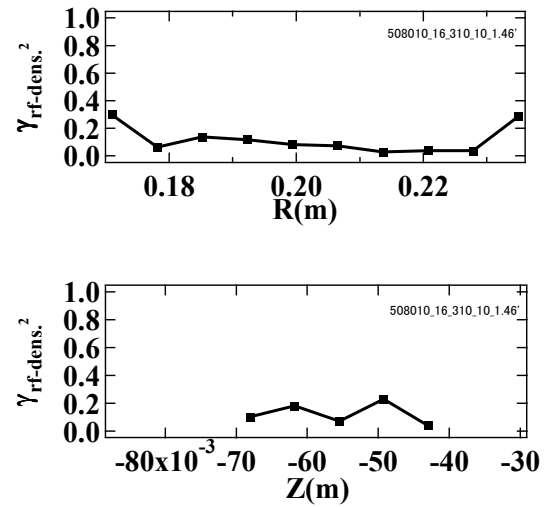


Fig.11 Radial and vertical profile of γ^2 ($f=1.4$ kHz) at $Z=-0.04$ m, and $R=0.22$ m, respectively

On the contrary, the S_{yy} and $\gamma_{rf-dens}^2$ at $B_z=2.2$ mT are shown in Fig12. S_{yy} shows several peaks at ~ 1.7 kHz, 3.2 and 5 kHz. $\gamma_{rf-dens}^2$ is > 0.8 at 1.7 kHz. As shown in Fig. 7 S_{xx} at the same frequency shows the coherent mode. Although the toroidal distance between measuring points is ~ 0.2 m, the wave number $k_{||}$ parallel to the magnetic field is thought to be ~ 0 , if the rf stray fluctuation is dominated by the density fluctuation.

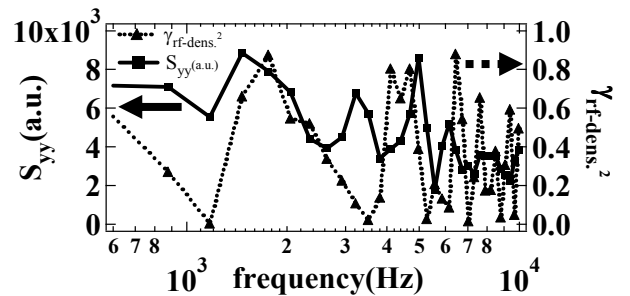


Fig.12 S_{yy} (line) and $\gamma_{rf-dens}^2$ (broken) spectra at $B_z=2.2$ mT

Figure 13 shown the vertical profile of $\gamma_{rf-dens}^2$ at $R=0.22$ m. If the cut off layer is extended vertically, which is expected from Fig. 3, the higher coherency in the vertical direction is understandable.

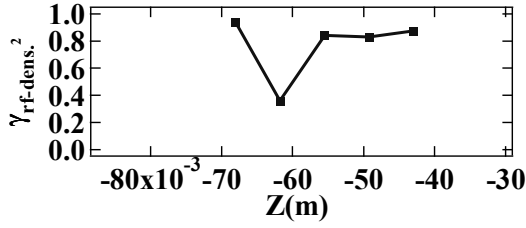


Fig.13 Vertical profile of γ^2 ($f=1.7$ kHz) at $R=0.22$ m

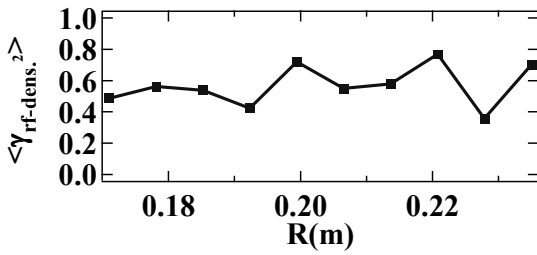


Fig.14 Line average radial profile of γ^2 ($f=1.7$ kHz)

This radial profile of $\gamma_{rf-dens}^2$ shows that the coherence is low near R_{res} and is high near the upper hybrid and R_{RC} (Fig.13). Figure14 shows line average radial profile of $\gamma_{rf-dens}^2$ at $f=1.7$ kHz. The $\gamma_{rf-dens}^2$ is $\approx 0.4 \sim 0.7$ at every measurement points. In the region where R_{CL} exists, the $\gamma_{rf-dens}^2$ varied from 0.7 to 0.4.

The cross phase spectrum between density fluctuation ($R=0.22$ m) and RF stray signal is shown in Fig15. The phase difference is about 100 degree at $f=1.7$ kHz. The S_{yy} shows the peak at the frequency correlation mode exists and also the $\gamma_{rf-dens}^2 > 0.7$ at that frequency.

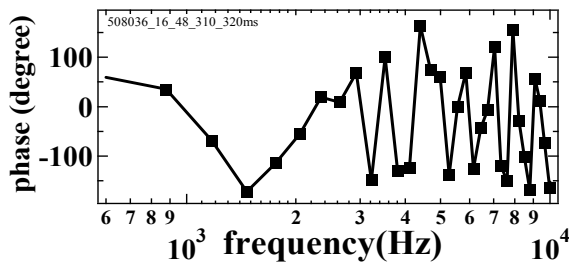


Fig.15 Phase spectrum between \tilde{n}_e and RF stray signal

4. Discussion and summary

In the BETA torus [19] a similar RF plasma using 2.45 GHz of ~ 0.7 kW has been studied at $B_T \sim 0.08$ T without B_z . Both density and potential fluctuations were measured by a scanning probe system. In the region of $R_{res} < R < R_{UHR}$ where $\vec{\nabla}n \cdot \vec{\nabla}B > 0$ co-existence of the

Rayleigh-Taylor and collisional drift are observed. The coherent mode is identified as RT mode near $R \sim R_{res}$ where $L_n \sim 0.05$ m. On the contrary near $R \sim R_{UHR}$ where $L_n \sim 0.12$ m but $\eta_e < 0$ low frequency modes at 2 and 4 kHz are found to be drift waves. Here $\eta_e = \nabla \ln T_e / \nabla \ln n_e$. As described in section 3-1, the coherent mode at $f=1.4$ kHz is found to extend over the region $R_{res} < R < R_{UHR} < R_{RC}$ and not to change its characteristics of coherency. Identification of this coherent mode is left for future.

In the TORPEX torus a transition from drift waves to interchange modes has been studied as a function of B_z/B_t [20]. Similar RF plasma was used and fluctuations are measured by multi probe systems around torus. The relationship between \tilde{n}_e and B_z have been investigated and reported. The density fluctuations were measured by probe array system with varied B_z . In the experimental results the maximum value of \tilde{n}_e/n_e is reduced by increasing of B_z . The integrated power of \tilde{n}_e in the frequency range ($0 \text{ kHz} < f < 40 \text{ kHz}$) was reduced with increasing of B_z and the power spectrum exhibits the peak at ~ 4 kHz up to 1.1mT. For increasing of B_z amplitude the wave number and frequency spectrum of \tilde{n}_e become narrow both in the ω - and in the k -space and peaks. The analysis results shown that the \tilde{n}_e weakly developed for every B_z . In our measurements the S_{xx} exhibits the peak at 1~2 kHz for even $B_z = 2.2$ mT.

In CDX-U the X-B mode conversion scenario has been studied by measuring the EB emission from the plasma and by comparing its fluctuating part with the density fluctuation measured by a scanning probe [6]. Observation shows that fluctuating L_n near the cut off layer is playing a role modifying the η_{XB} . The cross correlation between these signals was calculated in a time window of ~ 1 ms and 70 % anticorrelation was observed only in the region where the conversion occurred. No correlation was seen 2 cm on either side of this region. In our observations the correlation between the density and stray power fluctuations is only seen in the combination of B_z and B_T . Although it is difficult to interpret no coherence at $B_z = 0$, the tilting angle of the receiving horn antenna with respect to the toroidal field might be one of the reason. The high correlation at $B_z = 2.2$ mT around the upper hybrid and the cut off layer is consistent with those in CDX-U.

In summary, the 2D structure of density fluctuations is investigated in RF plasma with simple B_z/B_T magnetic configuration. The density profile is vertically elongated whose peak near R_{res} and L_n is ~ 0.04 m in the region of $R_{res} < R < R_{RC}$ where $\vec{\nabla}n \cdot \vec{\nabla}B > 0$. Correlation of the density fluctuation with stray RF power fluctuation which is expected to be reflected from the fluctuating cut off layer. At $B_z = 0$ mT although the coherent waves extending in the observable area (50×25 mm) are found to be excited in the low frequency range (1-10 kHz), $\gamma_{rf-dens}^2$ is found to be about 0.2. When $B_z = 2.2$ mT, the density

profile was kept almost constant, however, the relative fluctuation amplitude is reduced to 0.3 from 0.35. The radial correlation length is reduced to < 20 mm, but the vertical correlation length of ~ 25 mm is not changed. The peak in S_{yy} spectrum and $\gamma_{\text{rf-dens}}^2$ of 0.7 are observed at $f = 1.7$ kHz. The phase between \tilde{n}_e and RF stray signals is about 100 degree.

Acknowledgements

This work is partially performed with the support and under the auspices of the NIFS Collaboration Research Program (NIFS07K0AR009) and was supported by JSPS Grand-in-Aid for Scientific Research.

References

- [1] J. Preinhaelter and V. Kopecký *et al.*, J. Plasma Phys. **10**, 1 (1973).
- [2] H.P. Laqua *et al.*, Plasma Phys. Control. Fusion **49**, R1 (2007).
- [3] S. Shiraiwa *et al.*, Phys. Rev. Lett. **96**, 185003 (2006).
- [4] A. Pochelon, *et al.*, Nucl. Fusion **47**, 1552 (2008).
- [5] H.P. Laqua, *et al.*, Phys. Rev. Lett. **78**, 3467 (1997).
- [6] B. Jones, *et al.*, Phys. Rev. Lett. **90**, 165001 (2003).
- [7] F.F. Chen, *et al.*, Phys. Fluid **8**, 912 (1965).
- [8] F.F. Chen, *et al.*, Phys. Rev. Lett. **18**, 639 (1967).
- [9] A. Komori, *et al.*, Phys. Rev. Lett. **40**, 768 (1978).
- [10] T. Yoshinaga, *et al.*, 22nd IAEA FEC EX/P6-9, 2008.
- [11] T. Ryoukai, *et al.*, J. Plasma Fusion Res. **8**, 0105 (2009).
- [12] T. Yoshinaga, *et al.*, J. Plasma Fusion Res. **8**, 0100 (2009).
- [13] A. Huber, *et al.*, Plasma Phys. Control Fusion **47**, 409 (2005).
- [14] H. Zushi, *et al.*, Journal of Nuclear Materials **363**, 1386 (2007).
- [15] R. Bhattacharyay, *et al.*, phys. Plasmas **15**, 022504 (2008).
- [16] T. Kikukawa, *et al.*, J. Plasma Fusion Res. **3**, 010 (2008).
- [17] H. Zushi, *et al.*, Plasma Science and Technology **11**, 397 (2009).
- [18] F. F. Chen, 1984, Introduction to plasma Physics and Controlled Fusion, 2nd ed., Vol.1: "Plasma Physics" (Plenum Press, New York).
- [19] P K Sharma, *et al.*, Plasma Phys. Control. Fusion **39**, 1669 (1997).
- [20] F. M. Poli, *et al.*, phys. Plasmas **15**, 032104 (2003).